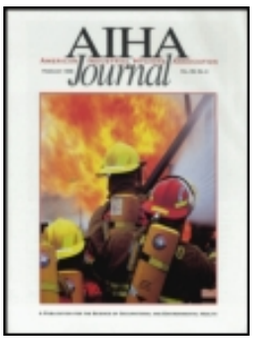

American Industrial Hygiene Association Journal

ISSN: 0002-8894 (Print) (Online) Journal homepage: http://www.tandfonline.com/loi/aiha20

Estimating the Contribution of Individual Work Tasks to Room Concentration: Method Applied to Embalming

James S. Bennett , Charles E. Feigley , Dwight W. Underhill , Wanzer Drane , Theresa A. Payne , Patricia A. Stewart , Robert F. Herrick , David F. Utterback & Richard B. Hayes

To cite this article: James S. Bennett , Charles E. Feigley , Dwight W. Underhill , Wanzer Drane , Theresa A. Payne , Patricia A. Stewart , Robert F. Herrick , David F. Utterback & Richard B. Hayes (1996) Estimating the Contribution of Individual Work Tasks to Room Concentration: Method Applied to Embalming, American Industrial Hygiene Association Journal, 57:7, 599-609, DOI: 10.1080/15428119691014648

To link to this article: http://dx.doi.org/10.1080/15428119691014648

Published online: 04 Jun 2010.

AMERICAN INDUSTRIAL HYGIENE ASSOCIATION JOURNAL 57:599–609 (1996)

Estimating the Contribution of Individual Work Tasks to Room Concentration: Method Applied to Embalming

AUTHORS
James S. Bennett[a]
Charles E. Feigley[a]*
Dwight W. Underhill[a]
Wanzer Drane[b]
Theresa A. Payne[b]
Patricia A. Stewart[c]
Robert F. Herrick[d]
David F. Utterback[e]
Richard B. Hayes[c]

[a]University of South Carolina School of Public Health, Department of Environmental Health Sciences, Health Sciences Building, Room 311, Columbia, SC 29208; [b]University of South Carolina School of Public Health, Department of Epidemiology and Biostatistics, Columbia, SC 29208; [c]National Cancer Institute, Environmental Epidemiology Branch, Bethesda, MD 20882; [d]Harvard School of Public Health, Department of Environmental Health, Boston, MA 02115; [e]National Institute for Occupational Safety and Health, Division of Surveillance, Hazard Evaluation and Field Studies, Cincinnati, OH 45226

A new approach for estimating emission rates from continuous concentration data was developed and applied to formaldehyde measurements collected during 25 embalmings. The instantaneous emission rate was estimated from the contaminant mass balance, which set the rate of emission equal to the sum of the rate of buildup in the room and the rate of removal in the exhaust flow. The generation rate of each specific work task was modeled using an equation that considered both the buildup and decay of the generation rate. Each term of the full modeling equation corresponded to a work task or event that occurred during the embalmings. The expected formaldehyde contribution of individual work tasks or events was then estimated by integrating each term using the gamma function. The work tasks or events with the largest formaldehyde contributions were aspiration of viscera after treatment with cavity fluid, embalming fluid spill, application of osmotic gel, and trocar cavity infusion. This analysis showed the relative importance of individual work tasks or events as contributors to the workroom formaldehyde concentration. This reconstruction of emission rates from concentration data is a general approach that may be used to proceed more effectively with control efforts in other processes where continuous data are available from reasonably well-mixed rooms.

Keywords: embalming, emission rates, exposure, formaldehyde, mathematical model, nonlinear regression

Continuous concentration data give more information on the influence of individual work tasks on room air contaminant concentration than does the time-weighted average (TWA) concentration. However, because concentration is affected by ventilation (i.e., dilution and convection), these data cannot be used directly to compare the emissions resulting from individual tasks or events. By calculating the contaminant generation rate using continuous concentration data and applying a mathematical model of the generation rate as a function of time after the occurrence of individual work tasks or events, this study develops a method to quantify the generation of a contaminant by individual work tasks. After this is done, the industrial hygienist can determine the relative contribution of individual work tasks to the contaminant concentration, and focus control efforts on the work tasks that cause emission of the largest amount of contaminant.

Many other investigators have modeled exposure hazards associated with air contaminant generating activities. To cite some recent examples, Nicas and Spear, using assumptions of exponential diffusion applied with known boundary conditions, predicted room concentrations of ethylene oxide resulting from a medical instrument sterilizing device.[1] Haberlin and Heinsohn, in modeling the movement of solvent vapors generated by a

*Author to whom correspondence should be addressed

Mention of any product or manufacturer does not constitute endorsement by the National Cancer Institute or the National Institute for Occupational Safety and Health.

coating operation within a bulk storage tank, applied a sequential box model incorporating evaporation and air exchange characteristics.[2]

The approach described here shares with these models the use of ventilation rate, mass balance principles, and mixing considerations to relate emission to concentration. But these earlier models used emission characteristics of sources to predict concentration. In contrast, this far more general approach uses solely the start time of each operation and the continuous concentration data to estimate the relative emission contributions of each source. The need for the type of procedure developed here is that in many operations, including embalming, the individual work tasks are so intertwined that they cannot be performed in isolation from each other. Therefore simply measuring the emission during an isolated operation is not possible.

The second point resolved in this article is that it is practical, even in a complex operation, to construct emission estimates based on the first derivative of the concentration with respect to time. In general, differentiation is a noisy operation in contrast with integration. The apprehension in using such an approach is that data from real operations are far too noisy to be of value. This was not the case with numerical differentiation of the data through Stirling's formula.

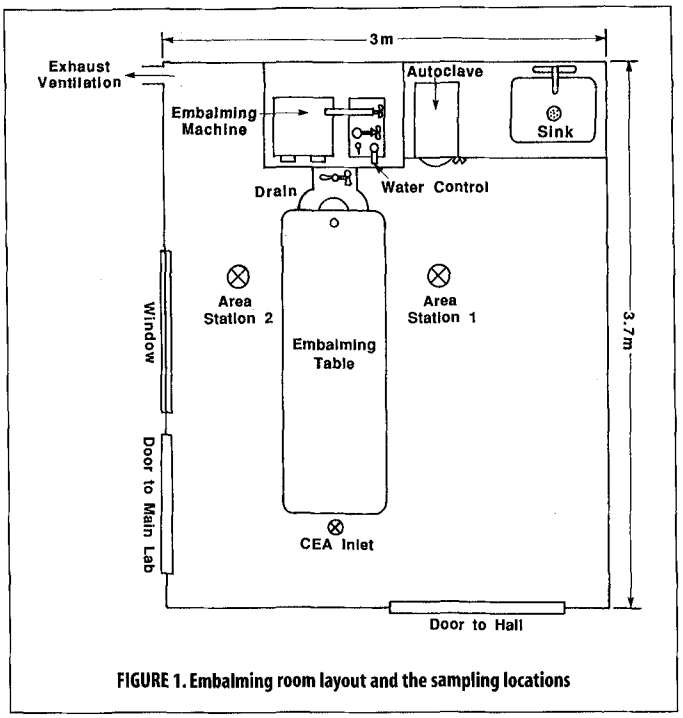

FIGURE 1. Embalming room layout and the sampling locations

METHODS

The steps in this analysis are (1) calculate the generation rate of formaldehyde using the ventilation rate and continuous concentration data; (2) model the generation rate using nonlinear regression analysis; and (3) compute the formaldehyde contribution of individual work tasks.

Data

The data used here were collected at the Cincinnati College of Mortuary Science under a contract titled "Industrial Hygiene and Biochemical Monitoring of Exposures Encountered by Embalmers," awarded to Azimuth Inc. from the National Cancer Institute, Environmental Epidemiology Branch. Stewart, et al. analyzed the results in a factorial study to evaluate the influence of case type (autopsied or intact), embalming fluid solution strength, and ventilation on formaldehyde concentration during 25 embalming experiments.[3]

Formaldehyde concentrations were monitored using a CEA TGM-555 (CEA Instruments, Inc., Emerson, N.J.) instrument with a data logger for continuous measurements and Occupational Safety and Health Administration (OSHA) Method 52 for both personal and area full-period, TWA formaldehyde concentrations. The limit of detection of the CEA instrument as set up for this experiment was 0.167 ppm formaldehyde. The CEA instrument logged a value every second. These values were then averaged over 10-second intervals to form the data set analyzed here. Figure 1 shows the embalming room layout and the sampling locations. The CEA instrument inlet was located at breathing zone height at the head of the embalming table. The vertical position of the area samples was approximately 0.7 m above the embalmer's head. One area sample (A1) was located horizontally at the embalmer's normal work station. The other area sample (A2) was symmetrically placed on the opposite side of the table, at a distance of about 1.5 m from A1. The distance between the CEA inlet and the area samples was approximately 2 m. The personal samples were collected on the embalmer's shoulder, outside the air-supplied hood. A complete description of data collection procedures may be found in Stewart et al.[3]

The dilution ventilation airflow rate was under experimental control. The three levels selected—low, intermediate, and high—corresponded to 0.51, 2.39, and 6.10 m^3/min. For the low ventilation level, the dilution airflow was due to supplied-air hoods worn by the embalmer and the industrial hygienists. Intermediate and high flow rates were measured at the face of the exhaust opening using a thermoanemometer (TSI Inc., St. Paul, Minn.) and verified with a flow hood (Shortridge Instruments) on the 1st, the 37th, and the 76th day of the study, and remained constant. The door to the embalming room was closed and sealed with duct tape during the experiments.[3] A list of work tasks thought to influence the contaminant generation rate was compiled prior to the experiment. An industrial hygienist observed each embalming and recorded the time of occurrence of each identified work task and other events, such as spills of embalming fluid, which could possibly generate airborne contaminants. From these records ASCII data files were created that contained a descriptive label for each work task or event, the time of occurrence, and the ventilation rate. Because the analysis was done at the level of individual procedures, some of which occur only during nonautopsied cases, some only during autopsied cases, and others in both types, the case type was not used directly in the data analysis. Also, case type and solution strength were not statistically significant determinants of the full-period TWA formaldehyde concentrations.[3]

Computation of Generation Rate

The formaldehyde generation rates were computed and the results displayed graphically using a program written in the Turbo Pascal (version 6.0) programming language. High resolution printed graphs were generated using Turbo Pascal to write printer command instructions via the HPGL/2 graphics language. The concentration data for each embalming were used numerically in the following equation, which yields the generation rate:

$$G = V\frac{dC}{dt} + QC \qquad (1)$$

where G is the instantaneous emission rate, mg/min; V is the room volume, m^3; Q is the ventilation rate, m^3/min; C is the contaminant

concentration mg/m³; and t is time, min. The room volume, V, in these tests was 26.6 m³. The derivative was approximated by the Stirling interpolation polynomial, shown in Appendix A.[4]

Application of Equation 1 requires the assumption that the room is well mixed. To determine the validity of this assumption in the embalming data, measurements taken at different room locations were compared by general linear model techniques. Also, Equation 1 assumes that no significant sinks for formaldehyde are present in the room.

Central to using the procedure presented in this article is a basic understanding of the mathematical methods used here. An interpolation polynomial is really a type of mathematical model of the data. To reduce truncation error, the derivative, dC/dt, was approximated numerically by the Stirling interpolation polynomial, which is a symmetric approximation based on the average of the forward and backward interpolation formulas of Gauss.[4,5] The Stirling polynomial is one of the most commonly used interpolation formulas utilizing central differences.[6] Equation 1 then produces a generation rate curve, G, which is a function of the event history of the embalming.

Modeling the Generation Rate

The second step in the analysis is to construct a mathematical model for the generation rate, based on the schedule of work tasks or events, using nonlinear regression analysis. On inspection of the generation rate, distinct peaks, which seemed to coincide with the occurrence of certain embalming work tasks or events, were observed. Also, some of these shapes had more than one peak, especially when two events overlapped. A function capable of imitating this complex behavior should have the following attributes: (1) a rise and fall triggered by a single event (as opposed to a rise triggered by one event and a fall triggered by another); (2) adjustable steepness; and, (3) additivity of the generation rate terms of each task or event.

With these criteria in mind, a model of the generation rate data was constructed using the function,

$$G = \sum_i u(t - t_i)k_i(t - t_i)^{\nu_i} e^{-\alpha_i(t-t_i)}, \qquad (2)$$

where

$$u(t - t_i) = \begin{cases} 0 \text{ if } t - t_i < 0 \\ 1 \text{ if } t - t_i \geq 0 \end{cases} \qquad (3)$$

Each term of the modeling equation corresponds, in theory, to an embalming work task or event. Thus, i indexes the work tasks or events. t_i is the time after the beginning of an embalming at which a work task begins. $u(t-t_i)$ is equal to zero until the work task begins and is equal to unity thereafter, at which time $t-t_i$ equals elapsed time since the beginning of the work task. In other words, the product $[u(t-t_i)] \cdot (t-t_i)$ functions as a clock that begins timing when event i occurs. Each event during the embalming has its own "clock." The k_i, ν_i, and α_i are parameters calculated in the nonlinear regression analysis that provide the best fit between model and data. In Equation 3 the k_i are scaling factors, the ν_i control the power function rise, and the α_i control the exponential decay.

To facilitate use of this equation, it was written in continuous form as follows:

$$G = \sum_i k_i \tau_i^{\nu_i} e^{-\alpha_i \tau_i}, \qquad (4)$$

where $\tau_i=[u(t-t_i)] \cdot (t-t_i)$.

The τ_i are equal to the time elapsed after the start of individual work tasks, and are zero until then. An individual term in this summation, G_i increases from zero until $\tau_i=\nu_i/\alpha_i$. Then, for larger values of τ_i, the exponential decay term dominates and G_i decreases back to zero in the limit. The ratio of ν_i to α_i controls the position of the peak maximum. The steepness of the peak is controlled by the magnitude of τ_i and α_i. A large ν_i causes a steep climb and a large α_i causes a steep descent.

The parameters, k_i, ν_i, and α_i, were adjusted to fit the corresponding peaks in the overall generation rate, G. The NLIN (nonlinear regression) procedure of the SAS/STAT software package (SAS Institute, Inc., Cary, N.C.) was used for this purpose.

The τ_i are found directly from the schedule of embalming procedures. Unlike the k_i, ν_i, and α_i, they are not estimated parameters. The generation rate, G, was found from the measured formaldehyde concentrations using Equation 1. The inputs to the NLIN procedure are the formaldehyde generation rate as a function of time and for each of the 42 unique tasks or events the values of the τ_i and the corresponding starting values for each of the parameters k_i, ν_i, and α_i. A modeling equation is specified (e.g., Equation 4), along with derivatives of this equation with respect to the parameters (k_i, ν_i, and α_i). The final values for these parameters are estimated by the NLIN procedure, using a least squares criterion, in such a way as to optimize the fit between the value of G predicted by the model and the value of G calculated from the data set. The resultant curve, which is the estimated generation rate function, is the sum of many individual wave forms of various shapes and sizes.

The following initial parameter values were used in the nonlinear regression: $k_i=0.036$, $\nu_i=9$, and $\alpha_i=6$. These values were used because they provided an approximate fit of the task-specific G(t) function to a section of a generation rate function calculated from the data, which occurred in isolation from other work tasks. The parameter estimates were constrained to be equal to or greater than zero to assist the NLIN procedure in converging to a physically reasonable solution. The ability of the modeling equation to fit the data was tested by applying the analysis to each of the 25 embalmings, singly. This was also useful for debugging and refining the SAS code and for finding anomalies in the data set. The least-squares parameter values, which resulted from running the model on the data for a single embalming, were used as the starting values for analysis of the complete data set.

The genuine power of this analysis is seen when the contribution to the generation rate of specific events or work tasks, such as "apply osmotic gel," is analyzed across the series of cases in which each occurs. Thus, to estimate the best fit value for each parameter, the regression model was applied to the entire data set of 25 embalmings. The NLIN procedure of the SAS programming language computes this set of parameter values, which provides the best fit between the generation rate for all 25 embalmings and the modeling equation. The product of this analysis is the set of parameter values that minimizes the error sum of squares; that is, the sum of the squares of the differences between the predicted G value and the G value calculated from the observed concentration at every data point. At this stage the modeling equation is completely determined and is unique to the data set.

Formaldehyde Contribution of Individual Work Tasks or Events

The focus now is on the individual terms of the summation, which represent the individual procedures or events. Integrating the

individual terms of the modeling equation gives the formaldehyde contribution of the corresponding work tasks. The integral of an individual term from its start to the end of the embalming is the total formaldehyde vapor contribution of a work task or event:

$$\gamma_i = \int_{\tau_i=0}^{\infty} k_i \tau_i^{v_i} \exp(-\alpha_i \tau_i) d\tau_i . \quad (5)$$

Infinity is used as the endpoint of the integration interval. The error from using infinity as the upper limit of integration instead of the end of the procedure is negligible because all the fitted generation rate curves enclose so little area beyond a procedure's end. This permits an analytical solution to the integral using the gamma function.[7]

RESULTS AND DISCUSSION

The degree of mixing within a room can be determined from the agreement of concentrations measured at different locations. Table I shows the analysis of variance (ANOVA) table for a general linear model using full-period TWA concentration as the dependent variable. The independent categorical variables were ventilation rate, case type, occurrence of spills, measurement location (CEA inlet, BZ, Area 1, or Area 2), and measurement location crossed with ventilation rate. Only ventilation rate, case type, and spill occurrence were statistically significant at the $\alpha=0.1$ level. The variables representing incomplete mixing, i.e., measurement location and measurement location crossed with ventilation rate, were not significant determinants of the measured concentration. Table II shows the Pearson correlation coefficients for full-period concentrations measured at the CEA inlet, Area 1, and Area 2 by ventilation level. Correlation coefficients for the BZ concentrations are reported only over all ventilation rates, because precise full-period values are known for just 11 of the 25 embalming experiments. Breaking this down into three ventilation classes results in very small sample sizes. Concentrations from different locations correlated well, especially under low ventilation conditions. Correlation coefficients for the medium ventilation rate condition are slightly lower and are lower still for the high ventilation rate. This is attributed to the fact that lower ventilation rates result in a longer residence time for eddy diffusion to reduce random concentration gradients within the room.

TABLE II. Correlation Coefficients of CEA Inlet, Breathing Zone, and Area Time-Weighted Average Formaldehyde Concentrations

Ventilation		CEA	Area 1	Area 2
Low	CEA	1	0.96	0.95
	Area 1		1	1.00
	Area 2			1
Intermediate	CEA	1	0.86	0.96
	Area 1		1	0.95
	Area 2			1
High	CEA	1	0.89	0.83
	Area 1		1	0.97
	Area 2			1

Ventilation		CEA	BZ	Area 1	Area 2
All	CEA	1	0.97	0.96	0.97
	BZ		1	0.94	0.96
	Area 1			1	0.99
	Area 2				1

Because the goal was to develop information for controlling worker exposure, the agreement between the concentration measured with the CEA and the concentration at the worker's breathing zone was the main concern. The mean formaldehyde concentration for the series of 25 embalmings measured with the CEA instrument was 2.70 ppm. The average full-period mean breathing zone (BZ) concentration, estimated by assuming a lognormal distribution to adjust for the measurements below limit of quantitation, was 2.6 ppm. Thus, the two means differed by only 4%, easily within the limits of measurement error.

The agreement between the CEA concentration and the BZ concentration for each period of the embalming also was investigated, because the embalmer's position with respect to both sources and the CEA sampling point varied somewhat by embalming period. Table III shows the ANOVA table for a general linear model using partial-period TWA concentration as the dependent variable. The independent categorical variables included ventilation rate, period, case type, measurement location (CEA inlet or BZ), measurement location crossed with period, and measurement location crossed with ventilation rate. Only period, ventilation rate, and case type were statistically significant at the $\alpha=0.1$ level. As in the analysis above, the variables representing incomplete mixing, i.e., measurement location, measurement location crossed with period, and measurement location crossed with ventilation rate, were not significant determinants of the measured concentration. The TWA concentrations measured at the four locations are shown in Table IV.

The model used here to relate concentration to emission rates assumes that the room is well mixed. A wide range of problems, such as dilution ventilation calculations and chemical reactor design, are approached by initially assuming the space is well mixed. In a completely

TABLE I. ANOVA Table of Full-Period Formaldehyde Concentration Measured at the CEA Inlet, Area 1, Area 2, and the Breathing Zone

Source	Degrees of Freedom	Type III Sum of Squares[A]	Mean Square	F Value	Pr > F
Measurement location	3	7.908	2.636	1.39	0.2507
Ventilation rate	2	182.856	91.428	48.28	0.0001
Case type	1	27.294	27.294	14.41	0.0003
Spill	1	28.210	28.210	14.90	0.0002
Measurement location crossed with ventilation rate	6	2.588	0.431	0.23	0.9666

[A]Type III sums of squares were used because the sample sizes differed slightly among levels of the variables. Type III sums of squares are independent of cell count, i.e., sample size.

TABLE III. ANOVA Table of Partial-Period Formaldehyde Concentration Measured at the CEA Inlet and the Breathing Zone

Source	Degrees of Freedom	Type III Sum of Squares[A]	Mean Square	F Value	Pr > F
Measurement location	1	3.079	3.079	0.42	0.5171
Period	3	484.424	161.475	22.16	0.0001
Ventilation rate	2	378.732	189.366	25.99	0.0001
Case type	1	20.382	20.382	2.80	0.0975
Measurement location crossed with period	3	8.014	2.671	0.37	0.7773
Measurement location crossed with ventilation rate	2	18.836	9.418	1.29	0.2790

[A]Type III sums of squares were used because the sample sizes differed among levels of the variables. Type III sums of squares are independent of cell count, i.e., sample size.

mixed room the concentrations of chemical species are uniform throughout. Mixing is never strictly complete in volumes with significant dilution flow and varying chemical generation rates. Undoubtedly, concentrations very close to emission sources in the embalming room were greater than the CEA measurements, and concentrations at the entry points of the dilution air were less than the CEA measurements. However, no significant differences in the concentrations were observed at the four monitoring locations. Evidence of rapid mixing of a contaminant plume under turbulence conditions similar to those in ventilated laboratories has been presented recently.[8] The plume concentration dropped by a factor of 10^4 after traveling only 60 cm at a velocity of 25 cm/sec. Also, because the concern here was with the impact of emissions on the embalmer's exposure, the agreement between the CEA and breathing zone measurements justifies the heuristic assumption of complete mixing for analysis of this experiment.

Figures 2 and 3 (Run 1 and Run 23) show examples of the formaldehyde concentration data and the estimated generation rates. Note that, although the concentration and generation rate are represented by unbroken lines as a visual aid, the data consist of 10-second averages. These particular runs were selected to represent the effects of the most important experimental variable, ventilation rate, over the range studied. The effect of the other two variables under experimental control, solution strength and type of case (autopsied or nonautopsied), on the TWA formaldehyde concentrations was not statistically significant.[3] The schedule of work tasks and their time of occurrence is shown along the horizontal axes. In Run 1 (Figure 2), at the low ventilation rate, the concentration built up in the room

TABLE IV. Summary of Formaldehyde Concentration TWAs[A]

Run	CEA FP	BZ FP[B]	Area 1 FP	Area 2 FP	CEA P1	BZ P1	CEA P2	BZ P2	CEA P3	BZ P3	CEA P4	BZ P4
1	2.60	2.87	2.46	2.64	0.09	nd	1.43	2.24	6.64	5.80	—	—
2	0.75	0.82	0.53	0.72	0.08	nd	0.73	0.67	1.00	1.00	—	—
3	1.09	1.41	0.87	1.30	0.10	nd	0.40	0.54	1.93	2.33	—	—
4	1.12	1.05	1.14	1.01	0.36	nd	0.71	0.27	2.11	2.14	—	—
5	4.14	4.07	2.93	3.26	0.66	0.36	2.84	2.38	6.45	5.74	13.15	13.26
6	0.81	0.33	0.23	0.28	0.38	nd	0.65	nd	1.33	0.48	—	—
7	1.75[C]	2.29	1.35	1.55	0.24	nd	1.28	1.51	3.28	3.12	3.09[C]	5.46
8	5.23	5.80–5.91	4.82	5.12	0.22	nd	2.64	3.97	9.08	9.33	—	—
9	2.22	2.27–2.39	1.37	1.66	0.14	nd	1.36	1.27	3.49	4.02	3.03	2.05
10	1.34	1.20–1.29	0.70	0.73	0.16	nd	0.88	1.00	1.91	1.67	—	—
11	2.62	0.57–0.69	1.74	1.90	0.44	nd	1.91	0.49	3.85	0.78	—	—
12	1.30	1.58–1.66	0.92	1.12	0.12	nd	1.19	2.05	1.83	1.66	—	—
13	1.09	1.22–1.33	0.93	1.02	0.03	nd	0.38	0.81	1.94	1.94	—	—
14	3.11	2.19–2.32	2.03	1.67	0.15	nd	1.73	1.76	5.60	3.60	—	—
15	2.34	2.79–3.14	2.79	2.24	0.26	nd	0.56	nd	6.52	8.85	—	—
16	10.30	8.67–8.78	7.52	8.15	0.13	nd	4.68	4.46	17.0	13.1	14.4	15.4
17	0.50	0.56–0.87	0.29	0.46	0.08	nd	0.22	nd	1.63	2.46	—	—
18	6.13	3.73–3.87	3.45	3.75	0.34	nd	4.04	2.99	10.47	5.84	9.38	6.11
19	4.49	4.83	3.06	3.24	1.76	7.03	3.55	2.75	6.94	5.28	4.02	12.89
20	5.14	5.51	3.17	3.55	1.28	0.66	3.03	3.54	11.59	12.57	—	—
21	4.99	4.14	3.54	3.78	0.68	0.60	5.31	5.10	8.26	6.10	9.43	7.29
22	0.47	1.70–2.07	1.28	1.26	0.26	nd	0.28	nd	0.95	5.77	—	—
23	1.14	1.33–1.42	0.63	0.82	0.02	nd	1.17	1.75	2.38	2.25	1.79	2.10
24	2.48	2.61	2.51	2.46	0.10	0.71	2.55	3.14	2.97	2.75	—	—
25	0.16	0.32–0.66	0.38	0.46	−0.19	nd	0.02	nd	1.04	1.42	—	—

[A]CEA, CEA instrument; BZ, breathing zone; FP, full-period TWA; nd, none detected; P1, . . . , P4, partial-period TWA for period 1, . . . , period 4
[B]For the BZ TWA when samples were below the limit of detection, a range is reported. The lower value assumes the undetected concentration to be zero. The higher value assumes the undetected concentration to be the limit of detection.
[C]CEA was inadvertently turned off two minutes early, thus missing a significant portion of the period with highest concentration.

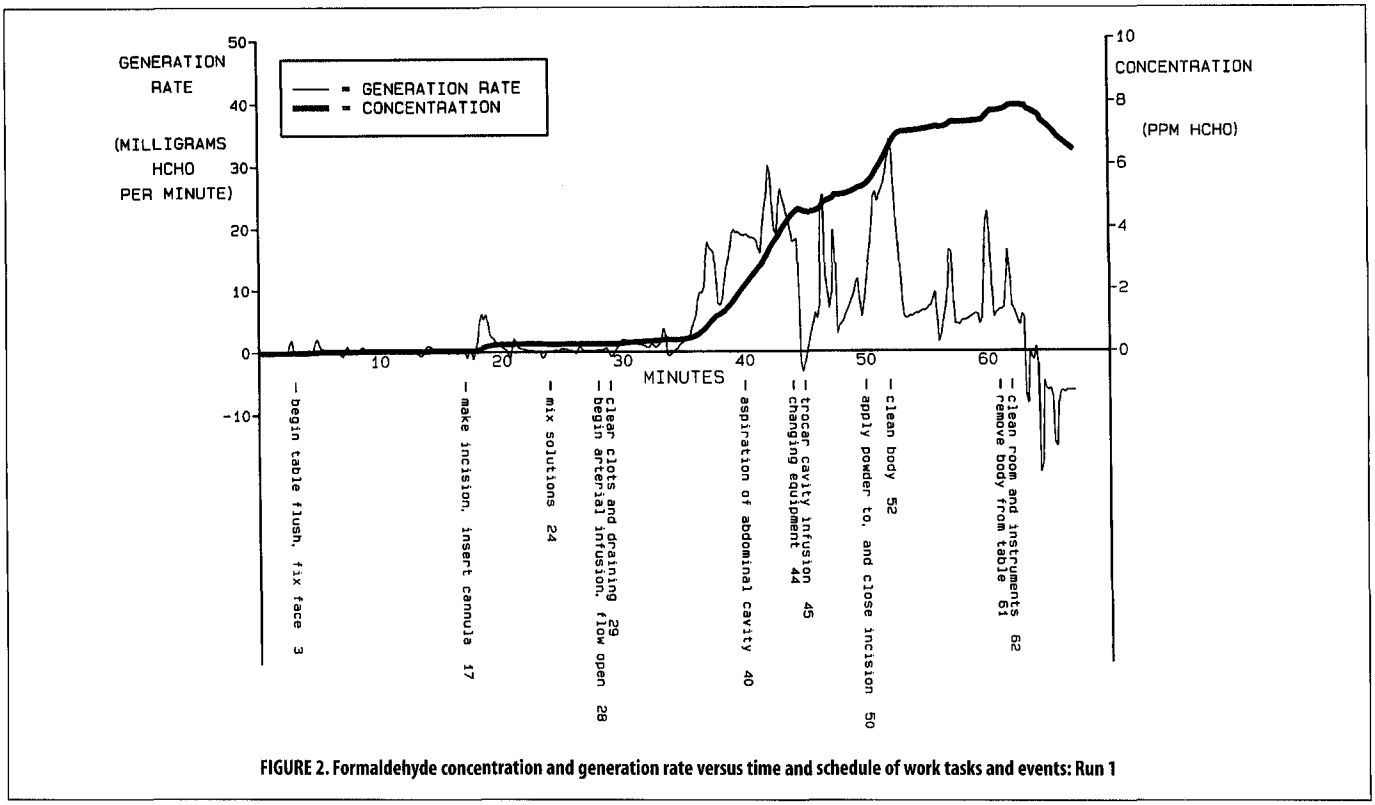

FIGURE 2. Formaldehyde concentration and generation rate versus time and schedule of work tasks and events: Run 1

after the work tasks with high formaldehyde generation rates began. A work task such as "trocar cavity infusion" (t=45 min) coincided with a slight increase in the formaldehyde concentration. However, this subtle change in concentration showed up dramatically in the generation rate curve. It is apparent that concentration data are not as helpful as the generation rate in identifying individual work tasks or events that emit formaldehyde.

Run 23 (Figure 3) shows the effects of the high ventilation rate. Even though formaldehyde emissions rates were as high as in Run

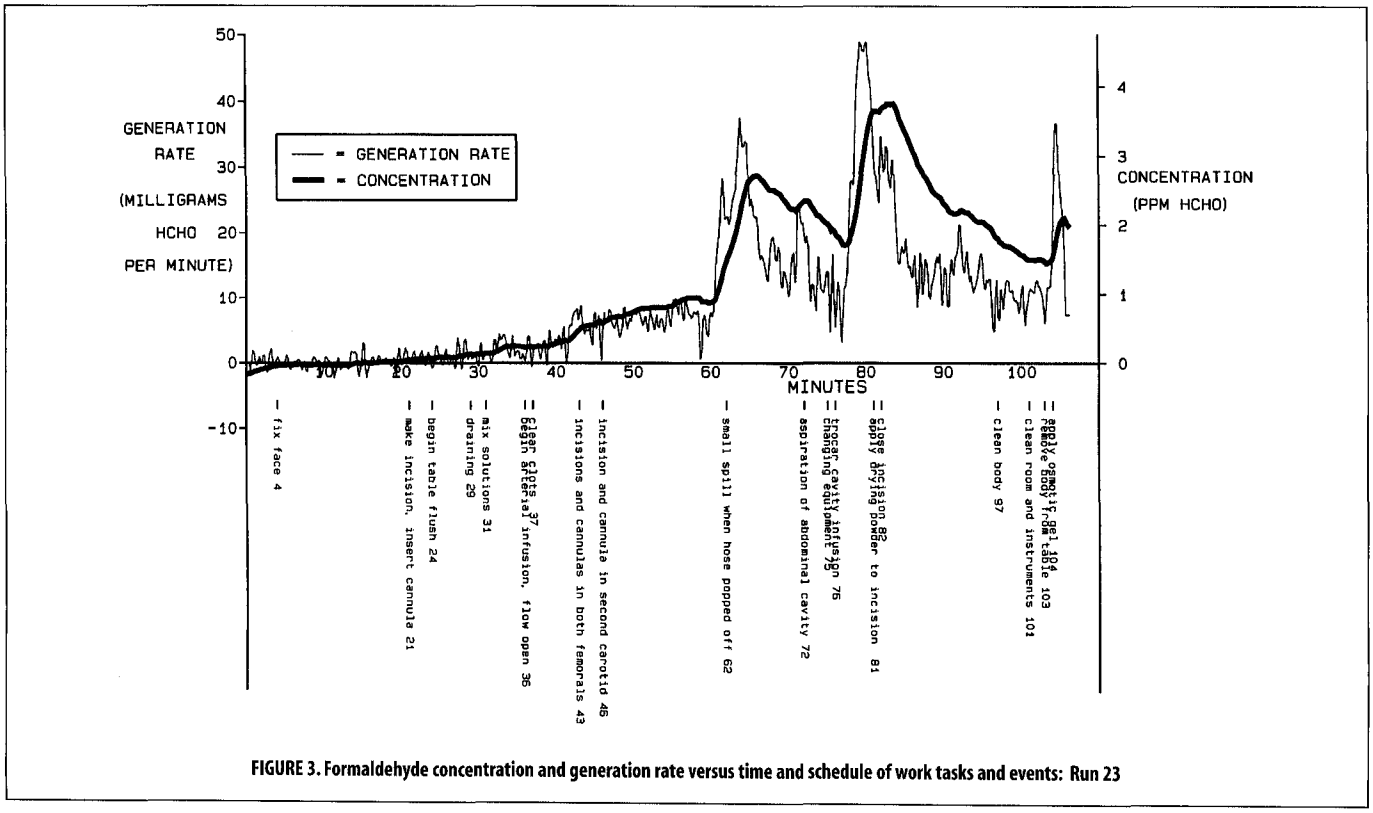

FIGURE 3. Formaldehyde concentration and generation rate versus time and schedule of work tasks and events: Run 23

TABLE V. Estimated Parameters of Formaldehyde Generation Rate Functions and Integrated Formaldehyde Contributions of Individual Embalming Work Tasks

Work Task or Event[A]	N/A[B]	n	k_i	ν_i	α_i	γ_i (mg CH_2O)
Aspirate viscera after cavity fluid	A	8	0.131	5.08	0.806	66
Embalming fluid spill	N,A	3	76.1	3.33	1.76	61
Osmotic gel applied	N,A	8	349	1.59	2.41	51
Trocar cavity infusion	N	12	55.7	19.3	7.38	41
Drying powder applied	N,A	20	49.8	2.13	1.60	26
Hardening compound applied	A	13	58.9	6.19	2.95	26
Close incision	N	12	0.0110	13.0	2.90	24
Mix solutions (third mix)	N,A	4	20.2	4.61	2.04	23
Treat viscera with cavity fluid	A	9	4.35	7.18	2.45	21
Final aspiration	A	13	151	8.44	4.36	14
Cauterize head cavity	A	10	281	4.45	3.63	12
Clean body	N,A	25	12.2	3.92	1.90	11
Close cavity	A	12	487	5.38	4.31	10
Apply plastic covering	N,A	6	1.49×10^3	2.96	6.06	6.9
Mix solutions (second mix)	N,A	14	262	2.62	3.95	6.9
Trocar chest wall	A	13	68.4	5.44	3.44	6.2
Aspirate from cavity	A	13	23.8	3.52	2.41	5.3
Aspiration of abdominal cavity	N	12	645	15.1	7.76	5.2
Prepare vessels with cannulae	A	13	42.8	1.36	3.58	2.6
Mix solutions (first mix)	N,A	25	0.306	2.62	0.82	2.3
Clean room and instruments	N,A	25	9.40×10^5	11.7	12.6	2.2
Fix face	N,A	23	85.9	16.1	7.670	1.8
Remove body from table	N,A	24	428	9.62	6.50	1.5
Suction fluids	N	4	1.96×10^4	10.5	7.72	1.4
Make incision, insert cannula	N	12	845	17.7	9.50	1.2
Arterial infusion	N,A	25	1.05×10^7	20.0	2930000	0.00
Clear clots	N	12	0.000	10.5	0.000	0.00
Draining	N	12	0.000	2.82	0.901	0.00
Changing equipment	N	12	0.000	10.8	0.000	0.00

[A] Parameters for the following work tasks were imprecise and are not included because the tasks were performed only once or twice over all the experiments: "Dryene" used in incision, "Dryene" applied topically, "Dis-spray" applied to mouth, trocar aspiration of cranial cavity, cauterize thoracic and abdominal cavity, osmotic gel applied to face and hands, trocar infusion of buttocks, nasal aspiration, trocar infusion of lower legs, make femoral incision and second femoral incision.

[B] Type of embalming in which work task or event occurred: A = autopsied cases; N = nonautopsied cases

1, the concentration did not build up continuously, because the rate of removal in the exhaust air was much higher than in Run 1. Nevertheless, the generation rates were high enough that the OSHA short-term exposure limit was exceeded at the high ventilation rate. Also, the generation rate curve shows a great deal more variability than the generation rate in Run 1. This is probably because the room was less well mixed at higher ventilation rates, producing greater short-term random variation in concentration than in Run 1. This variability is amplified somewhat by taking the derivative to calculate the generation rate.

Table V gives the best fit parameter values for the nonlinear regression using the model in Equation 2. The work tasks for which k_i was estimated to be zero made no discernible contribution to formaldehyde in workroom air. Eleven of the 42 work tasks occurred only once or twice over all 25 experiments. Thus, their parameter estimates were judged to be inaccurate and are not included in Table V. Some of these 11 tasks involved use of products that contain no formaldehyde (i.e., Dryene and Dis-spray).

Figures 4 and 5 show the generation rate data and the model predictions from Equation 2 when fit to data from all 25 runs. The peaks in the model are controlled by the timing of the observed work tasks. Because each term of the model was switched on only when the corresponding event occurred, the model was incapable of following a peak in generation rate if no event coincided with the peak. This may occur because some emissions resulting from a particular task may not occur until some time after the task was initiated, or the industrial hygienist observing the procedures may have missed reporting a significant task or event. Also, the mathematical form of the model may not fit well the generation rates of each task. Some tasks may produce multiple generation peaks (e.g., the aspiration of abdominal cavity shown in Figure 4), or their shape may be irregular. Another explanation for deviations of the model predictions from the generation rate data is that most tasks were performed in more than one embalming, and the generation rates for a particular task varied somewhat each time the task was performed. For instance, the generation rate and total amount resulting from a spill of embalming fluid will vary greatly depending on the amount spilled, the solution strength, the temperature, the humidity, and the airflow over the spill. Fitting the model over all runs produces a single set of parameters for each task that best characterizes the generation rates of that task over all occurrences.

Even though a better fit could be obtained by fitting each occurrence separately, the aim was to reduce these data to a single set of parameter values for each task, so that the tasks contributing the most formaldehyde to room air could be identified and potentially controlled. Thus, the objective was not to fit each peak perfectly, but to obtain an averaged contribution for each task over these 25 experiments.

Integrating an individual term for work task "i" in Equation 2 over time yields γ_i, the average mass contribution for that work task. For example, the average mass contribution of Task 23, osmotic gel applied, is:

$$\gamma_{23} = \int_{\tau_{23}=0}^{\infty} 349\, \tau_{23}^{1.59} \exp(-2.41\, \tau_{23}) d\tau_{23}$$

$$= 51.0 \text{ mg, } CH_2O$$

Appendix B illustrates this integration in detail.

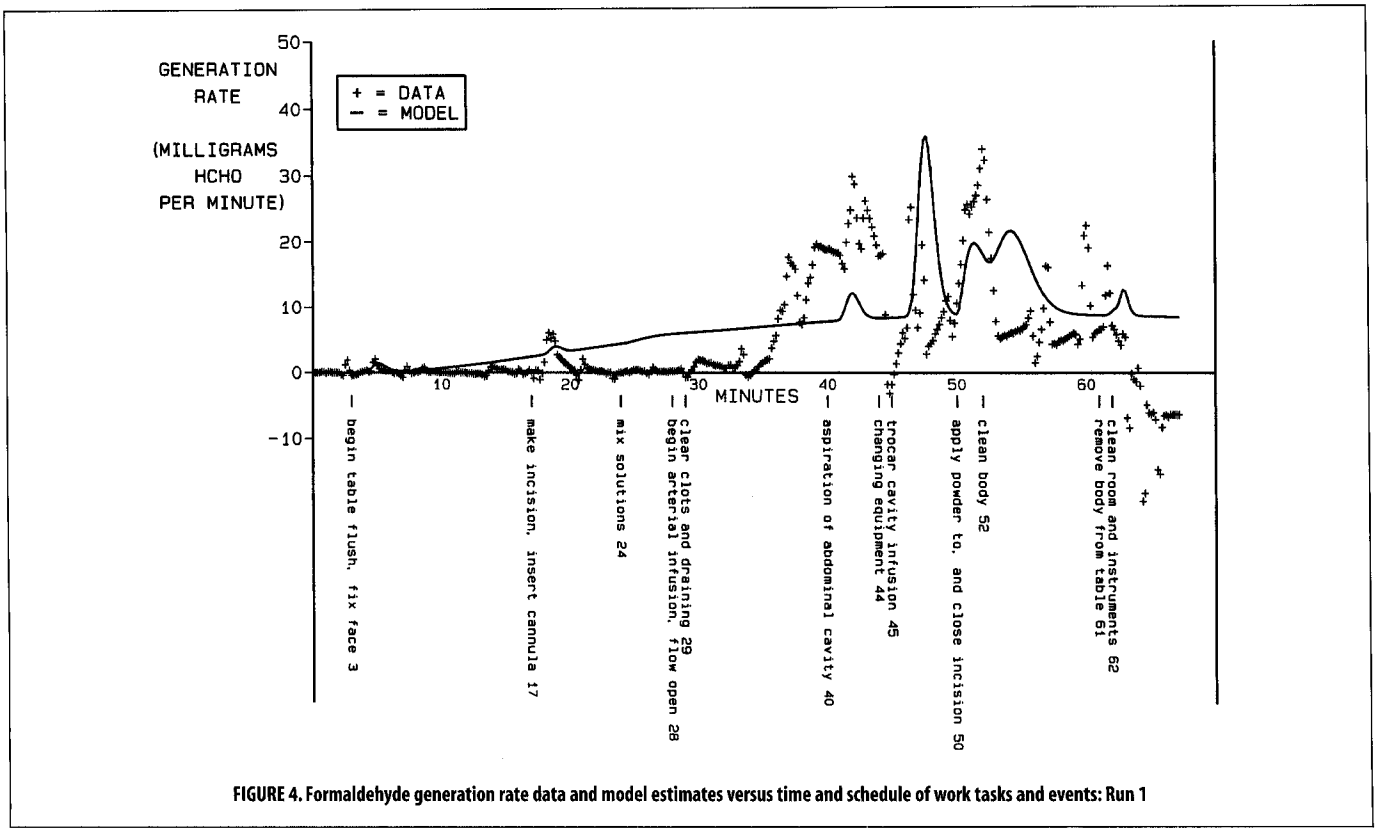

FIGURE 4. Formaldehyde generation rate data and model estimates versus time and schedule of work tasks and events: Run 1

The mass contributions for each work task, given in Table V, may be used to focus control efforts on the procedures that emit the most formaldehyde to room air. The aspiration of viscera after treatment with cavity fluid, occurring only during autopsied cases, was the largest formaldehyde emitter, and trocar cavity infusion with cavity fluid, occurring only during nonautopsied cases, emitted the fourth largest amount. Cavity fluid has a high formaldehyde concentration and, unlike arterial fluid,

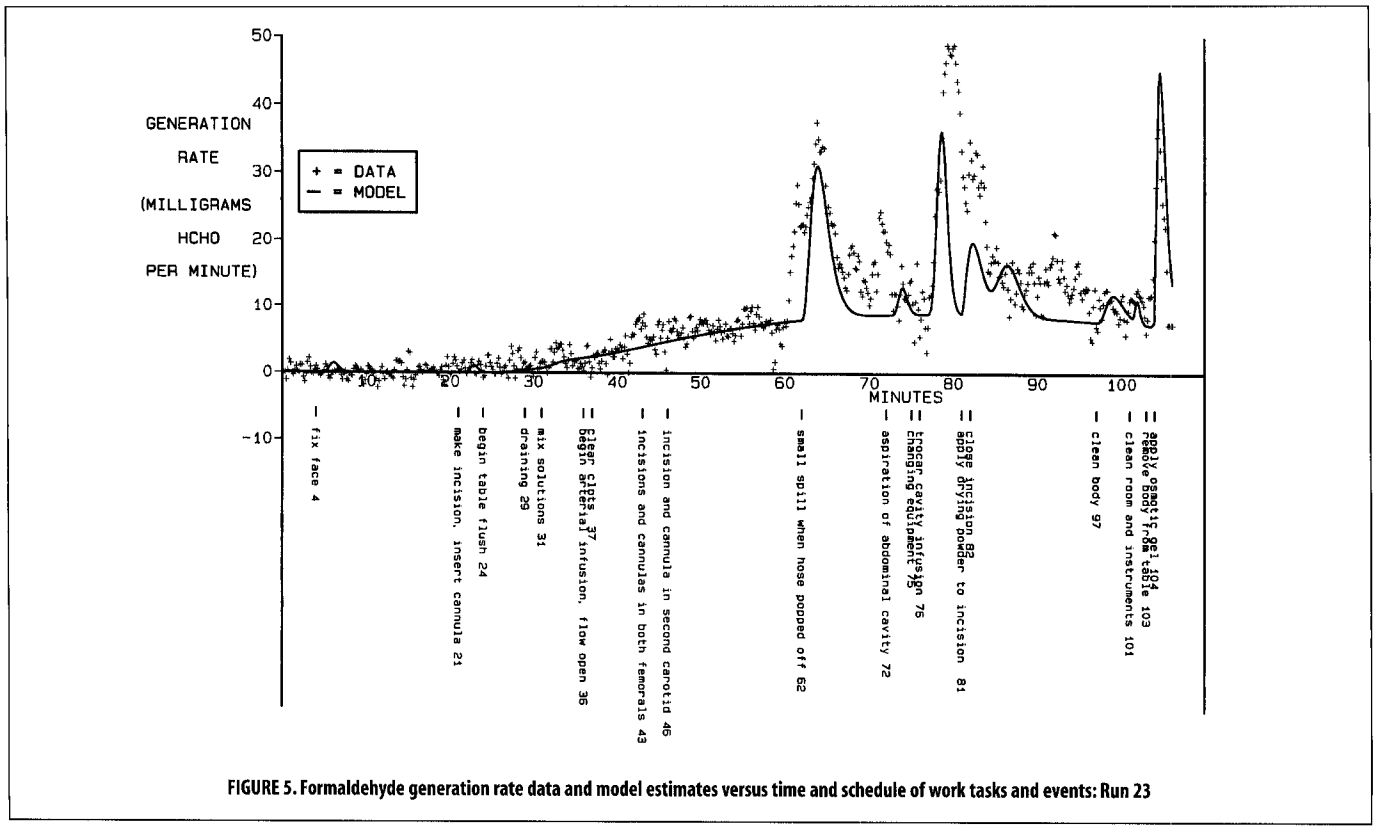

FIGURE 5. Formaldehyde generation rate data and model estimates versus time and schedule of work tasks and events: Run 23

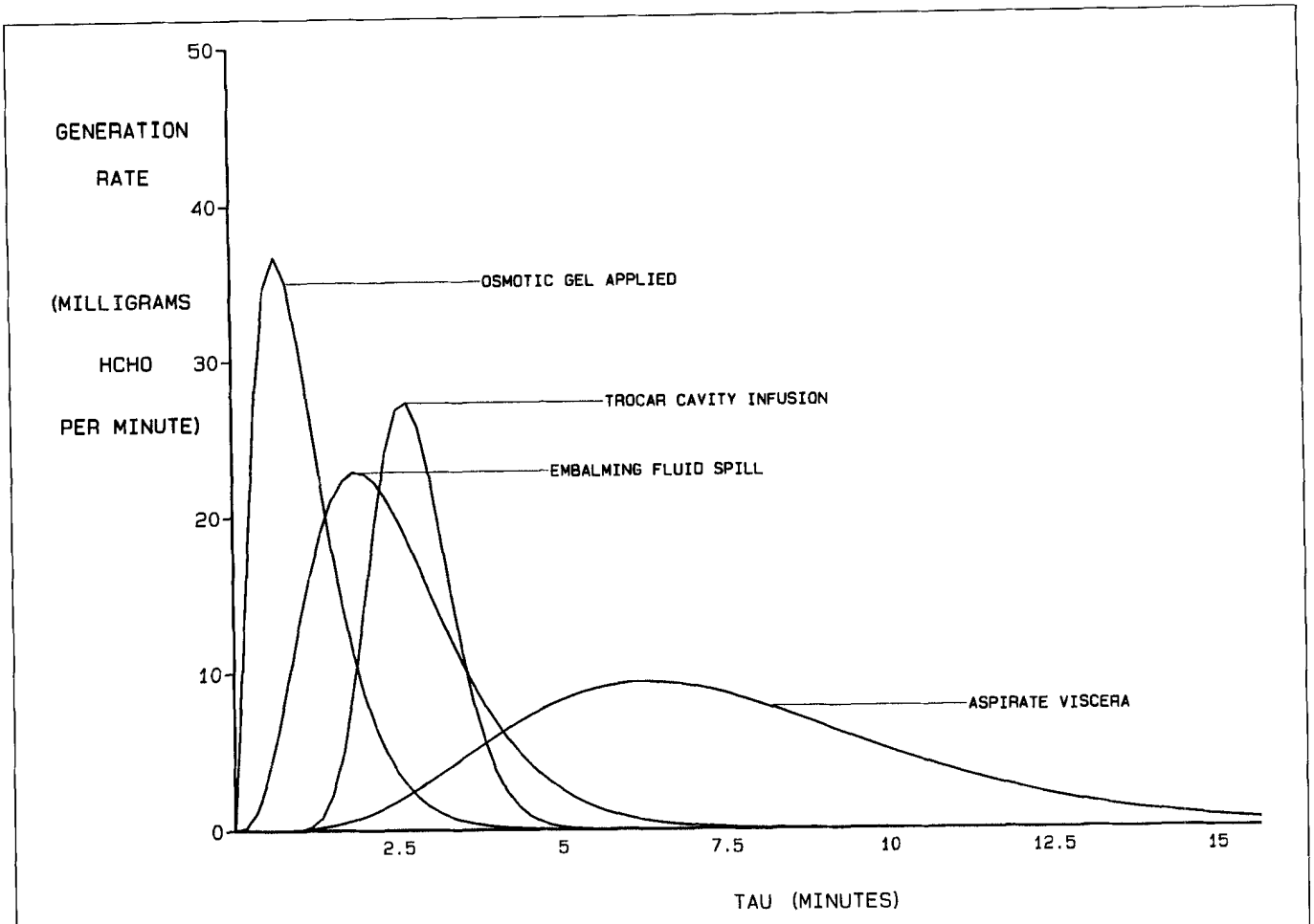

FIGURE 6. Model estimates of formaldehyde generation rates for individual work tasks and events

is not diluted prior to use. In autopsied cases treatment of viscera was performed in a plastic bag that was not tightly sealed ("treat viscera with cavity fluid") and excess fluid was sucked from the bag ("aspirate viscera") using a water aspirator discharging to an open sink. It is not clear if the bag, the aspirator, or both emit formaldehyde to room air. For either source, local exhaust ventilation may prove an effective control approach.

The use of other products containing formaldehyde, including osmotic gel, drying powder, and hardening compound, contributed significant quantities of formaldehyde to room air. These products generally are used on the embalming table, suggesting that local exhaust of the table could be an effective control measure. Nevertheless, fluid spills on the floor represented the second most important source and can only be controlled through good work practices, including immediate clean up of spilled fluids with material capable of permanent sorption or chemical destruction of formaldehyde.

Interestingly, the mixing and infusion of arterial fluids, which were used in liter quantities during all embalmings, emitted much less formaldehyde than the use of various special purpose products in much smaller amounts. This agrees with the findings of personal exposure monitoring.[3] Although arterial fluid leaving the body is drained onto the table, its formaldehyde concentration may be reduced in passage through the body by reaction with tissues. Also, a water flush of some table surfaces may reduce the amounts of formaldehyde emitted. While mixing of embalming fluid solutions made a relatively small contribution to room formaldehyde levels, it is noteworthy that integrated emission increased from the first mix through the third mix, as indicated in Table V. This may be due to the use of different fluids and different fluid strengths as the embalmings proceeded.

A distinctive feature of the model is the variety of peak shapes, from narrow to wide mounds, overlapping in complex combinations, which the exponential terms in the summation in Equation 2 produce. Figure 6 shows the generation rate curves fitted to some of the tasks or events with the largest formaldehyde emissions. In addition to the time integrated mass emission, the duration and peak level of emission are important determinants of exposure. Such figures may be used to determine the type of exposure limit—8-hour TWA, short-term exposure limit (STEL), or ceiling—most relevant to the occurrence of a work task and how the exposure might best be controlled.

The aspiration of viscera had a higher integrated contribution than use of osmotic gel (Table V). However, comparison of the fitted emission rate curves of these two tasks in Figure 6 shows that, averaged over all runs, emissions from viscera aspiration were spread out over 15 minutes, while most of the formaldehyde emission from osmotic gel occurred within 2 minutes of application, and the peak generation rate for osmotic gel was about four times higher than for viscera aspiration. If the peak concentration is a more important determinant of health impact than the TWA, then controlling emissions from osmotic gel should be given a higher priority than controlling emissions from viscera aspiration. In general, brief, intense bursts like those from osmotic gel application have greater

potential to exceed ceiling limits than more gradual emissions, such as those from viscera aspiration, when at least some degree of dilution ventilation is maintained.

Interpretation of the nonlinear regression results must be approached cautiously. For this series of embalming experiments, the first task in all the embalmings, starting the table flush with tap water, was estimated to have a slowly increasing, very broad emission rate curve with a high integrated mass contribution. However, there is no reason to believe that flushing the table with water causes formaldehyde emissions. Indeed, table flush may actually reduce the effective emission rates of other tasks. There is no rise in the formaldehyde level that corresponds to the beginning of the table flush. However, because it is the first task in every experiment, its term in Equation 2 unintentionally serves to account for changes in the baseline formaldehyde levels that are not accounted for by the net effect of all the other terms. Similarly, the task "sealing putty used in head cavity" would not be expected to emit formaldehyde, because sealing putty contains no formaldehyde. Sealing putty was used during only one embalming experiment and occurred about 5 minutes before a peak in the formaldehyde emissions that corresponds to final aspiration. In that experiment the final aspiration emission rate was higher than in other experiments. Thus, the model fitted to data from all the experiments underestimated the final aspiration emission rate for this experiment and assigned the emission rate excess to the task that occurred just before final aspiration, i.e., sealing putty used in head cavity. Because sealing putty was used only once, the confounding influence of final aspiration was not offset by emission rate data from other embalming experiments. Thus, the "table flush" and "sealing putty" terms were not reported in Table V because they are believed to be artifacts that do not represent the true effect of these tasks.

CONCLUSION

While graphs of concentration versus time may give an industrial hygienist some insights into the control of complex, multisource processes, the graphs of generation rates versus event occurrence time, as shown here for embalming, are a more sensitive tool for analyzing such work procedures. The mathematical model that characterizes each task individually based on its contaminant generation rate provides an excellent means of comparing the relative hazard associated with various work tasks and events.

The ranking and characterization of emission may be used to identify the work tasks that require the application of control measures, to determine the type of exposure limits (i.e., 8-hour TWA, STEL, or ceiling) most likely to be exceeded, and to gain insight into how exposure is best controlled. Products and materials that emit large amounts of contaminants could be replaced with suitable substitutes. Process modifications may be pursued based on the identification of hazardous work tasks. It may be possible to enclose or isolate processes emitting large quantities of contaminant. Activities that emit contaminants at high rates from localized areas may be controlled through local exhaust ventilation, while those tasks emitting contaminants at low rates from many locations may be controlled through dilution ventilation. Also, the identification of sources and estimation of their emission rates could be used to develop an administrative control plan. If other measures are not feasible, then the kinds of information developed here would be helpful in selecting respiratory protection and determining the required protection factor.

Given a representative series of concentration and event data, it would be possible to estimate using this approach the concentration profile over time of any hypothetical sequence of these events. TWA concentrations and peak concentrations may then be easily calculated to judge compliance of a planned schedule of work tasks and a dilution ventilation rate with exposure limits.

Industrial hygienists historically have collected concentration data. By using the differential mass balance, they can reconstruct the actual emission rates of contaminants by individual tasks or events and proceed more effectively with control recommendations. This reconstruction of emission data from concentration data is a general procedure and should have widespread application where continuous concentration data are available from reasonably well-mixed spaces.

The embalming experiments were performed before this analytical approach was developed. Such *a posteriori* analyses may suffer from the failure to recognize important tasks and events during data collection. When applying the method described here, video recording of all work practices is strongly recommended, in conjunction with continuous air monitoring. Also, independent laboratory verification of work task emission characteristics in isolation is desirable whenever possible, although this was not done in the present study. Interested parties may contact the principal author to obtain the database formats and SAS and Turbo Pascal programs used in this analysis and for assistance with their application.

REFERENCES

1. **Nicas, M. and R.C. Spear:** Application of mathematical modeling for ethylene oxide exposure assessment. *Appl. Occup. Environ. Hyg. 7*:744–748 (1992).
2. **Haberlin, G.M. and R.J. Heinsohn:** Predicting solvent concentrations from coating the inside of bulk storage tanks. *Am. Ind. Hyg. Assoc. J. 54*:1–9 (1993).
3. **Stewart, P.A., R.F. Herrick, C.E. Feigley, D.F. Utterback, et al.:** Study design for assessing exposures of embalmers for a case-control study. Part I. Monitoring results. *Appl. Occup. Environ. Hyg. 7*:532–540 (1992).
4. **Demidovich, B.P. and I.A. Maron:** *Computational Mathematics.* Moscow: MIR Publishers, 1981. pp. 580–583.
5. **Kunz, K.S.:** *Numerical Analysis.* New York: McGraw-Hill, 1957. pp. 66–85, 125–136.
6. **Hornbeck, R.W.:** *Numerical Methods.* New York: Quantum Publishers, 1975. pp. 41, 121.
7. **Abramowitz, M. and I.A. Stegun (eds):** *Handbook of Mathematical Functions.* New York: Dover Publications, Inc., 1970. p. 255–257.
8. **Rhodes, C.E., R.M. Kamens, and R.W. Wiener:** Experimental considerations for the study of contaminant dispersion near the body. *Am. Ind. Hyg. Assoc. J. 56*:535–545 (1995).

APPENDIX A

The numerical differentiation formula based on the Stirling interpolation polynomial approximates the derivative of y with respect to x as follows:

$$\frac{dy}{dx} = \frac{1}{h}\left(\Delta y_{-1/2} + q\Delta^2 y_{-1} + \frac{3q^2-1}{6}\Delta^3 y_{-3/2} + \frac{2q^3-q}{12}\Delta^4 y_{-2} + \frac{5q^4-15q^2+4}{120}\Delta^5 y_{-5/2} + \frac{3q^5-10q^3+4q}{360}\Delta^6 y_{-3} + \ldots\right),$$

where $q = (x - x_0)/h$ and $h = x_{i+1} - x_i$ $(i = 0, 1, 2, \ldots)$.

TABLE IA. Illustration of the Δ-Notation

Index i	t	C	ΔC	Δ^2C	Δ^3C	Δ^4C	Δ^5C
−3	.167	2.015					
			0.985				
−2	.333	3.000		−0.445			
			0.540		0.165		
−1	.500	3.540		−0.280		0.055	
			0.260		0.220		−0.265
0	.667	3.800		−0.060		−0.210	
			0.200		0.010		0.150
1	.833	4.000		−0.050		−0.060	
			0.150		−0.050		
2	1.00	4.150		−0.100			
			0.050				
3	1.167	4.200					

The most accurate estimate is obtained when the derivative is evaluated at the center of the interpolation interval. Therefore, setting $x=x_0$:

$$\frac{dy}{dx} = \frac{1}{h}\left(\Delta y_{-1/2} + \frac{-1}{6}\Delta^3 y_{-3/2} + \frac{1}{30}\Delta^5 y_{-5/2} + \ldots\right).$$

Using the notation for concentration:

$$\frac{dC}{dt} = \frac{1}{h}\left(\Delta C_{-1/2} + \frac{-1}{6}\Delta^3 C_{-3/2} + \frac{1}{30}\Delta^5 C_{-5/2} + \ldots\right)$$

where $\Delta C_{-1/2} = (\Delta C_{-1} + \Delta C_0)/2$, $\Delta^3 C_{-3/2} = (\Delta^3 C_{-2} + \Delta^3 C_{-1})/2$, and $\Delta^5 C_{-5/2} = (\Delta^5 C_{-3} + \Delta^5 C_{-2})/2$.

The Δ-notation is illustrated by Table IA.

The derivative dC/dt evaluated for time t=0.667 of the example concentration function shown in Table IA is approximated as:

$$\frac{dC}{dt} = \frac{1}{0.1667}\left(\frac{0.260 + 0.200}{2} - \frac{1}{6}\left[\frac{0.220 + 0.010}{2}\right] + \frac{1}{30}\left[\frac{-0.265 + 0.150}{2}\right] + \ldots\right) \approx 1.25 \frac{\text{mg/m}^3}{\text{min}}$$

APPENDIX B

The integral form of the gamma function is as follows:[7]

$$\Gamma(z) = \int_0^\infty t^{z-1}e^{-t}\,dt = \omega^z \int_0^\infty t^{z-1}e^{-\omega t}\,dt, \text{ for } z > 0.$$

This can be written in a form that is convenient for solving Equation 5 through a change of variables:

Let $z'=z-1$. Then, $z=z'+1$, and:

$$\Gamma(z' + 1) = \omega^{z'+1} \int_0^\infty t^{z'}e^{-\omega t}\,dt.$$

The gamma function has the following property:[7] $\Gamma(z'+1)=z'\Gamma(z')$.

We now have:

$$\frac{z'\Gamma(z')}{\omega^{z'+1}} = \int_0^\infty t^{z'}e^{-\omega t}\,dt.$$

Using the notation of Equation 5:

$$\frac{\nu_i\Gamma(\nu_i)}{\alpha_i^{\nu_i+1}} = \int_0^\infty \tau_i^{\nu_i}e^{-\alpha_i\tau}\,d\tau_i, \text{ for } i = 1, 2, \ldots, 42.$$

Incorporating the k_i parameter is handled easily, as it involves simply the multiplication by a constant:

$$k_i \frac{\nu_i\Gamma(\nu_i)}{\alpha_i^{\nu_i+1}} = k_i \int_0^\infty \tau_i^{\nu_i}e^{-\alpha_i\tau}\,d\tau_i = \int_0^\infty k_i\tau_i^{\nu_i}e^{-\alpha_i\tau}\,d\tau_i = \gamma_i$$

Turning again to Stirling, the gamma function is approximated by:

$$\Gamma(z) = e^{-z}z^{(z-1/2)}(2\pi)^{1/2}\left[1 + \frac{1}{12z} + \frac{1}{288z^2} - \frac{139}{51840z^3}\right],$$

for z large and positive.[7]

For z small and positive, the gamma function of z is available in tables.

Using the notation of Equation 5:

$$\Gamma(\nu_i) = e^{-\nu_i}\nu_i^{(\nu_i-1/2)}(2\pi)^{1/2}\left[1 + \frac{1}{12\nu_i} + \frac{1}{288\nu_i^2} - \frac{139}{51840\nu_i^3}\right].$$

As an example, the formaldehyde contribution of the application of osmotic gel (Work Task 23) is estimated as:

$$\gamma_{23} = \int_{\tau_{23}=0}^\infty 349\,\tau_{23}^{1.591}\exp(-2.408\,\tau_{23})d\tau_{23}$$

$$= 349\,\frac{1.59\Gamma(1.59)}{2.41^{(1.59+1)}} = 349\,\frac{1.59(0.89243)}{2.41^{2.59}}$$

$$= 51 \text{ milligrams } CH_2O.$$

Note: 72.7°F is the average room temperature during the embalming experiments.